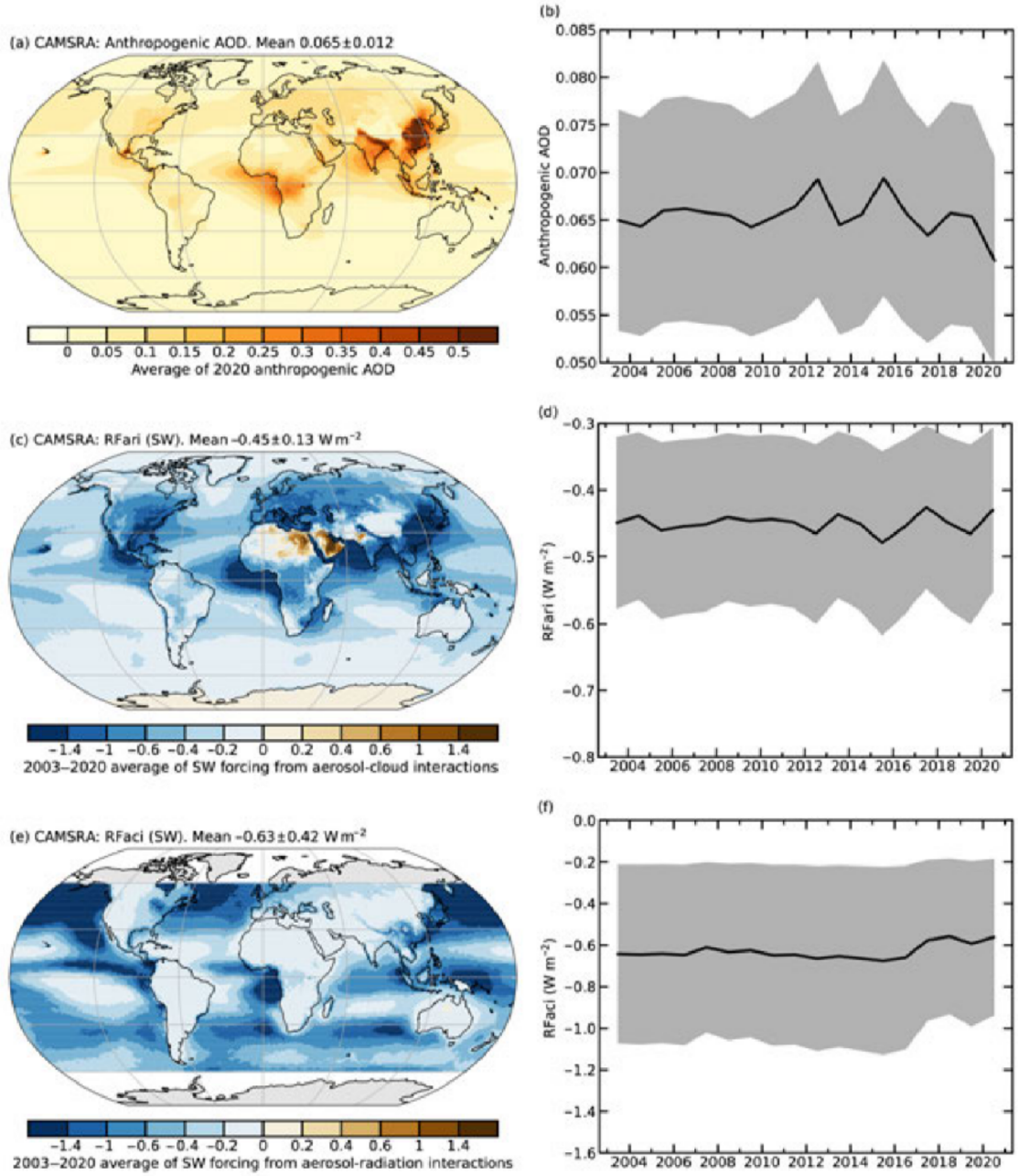

Fig. 2.56. CAMSRA (a) 2020 average of anthropogenic aerosol optical depth (AOD); (b) global annual average of anthropogenic AOD from 2003 to 2020. Radiative forcing in the shortwave (SW) spectrum due to (c),(d) aerosol-radiation (RFari) and (e),(f) aerosol-cloud interactions (RFaci). The left column shows the average distribution for the period 2003–20. The right column shows time series of global averages for the same period, with the 1-σ uncertainties of these estimates shown in gray.

4) Stratospheric ozone—M. Weber, W. Steinbrecht, C. Arosio, R. van der A, S. M. Frith, J. Anderson, L.Castia, M. Coldewey-Egbers, S. Davis, D. Degenstein, V. E. Fioletov, L. Froidevaux, D. Hubert, D. Loyola, C. Roth, A. Rozanov, V. Sofieva, K. Tourpali, R. Wang, and J. D. Wild

Stratospheric ozone protects Earth's biosphere from harmful ultraviolet (UV) solar radiation. The total ozone column determines how much UV reaches the surface. Most of the ozone resides in the lower stratosphere ("ozone layer"), where it is recovering slowly from anthropogenic Ocean Depleting Substances (ODS). Clearer signs of ozone recovery, due to the phase-out of ODSs mandated by the Montreal Protocol in the late 1980s (section 2g2), are seen in the upper stratosphere (WMO 2018).

The year 2020 was remarkable because the annual mean anomaly of total column ozone was negative for most of the globe (Plate 2.1aa). This negative anomaly was due to the combination of

very low polar ozone during Arctic winter/spring (Manney et al. 2020; Inness et al. 2020; Dameris et al. 2021) and a large and unusually long-lasting Antarctic ozone hole (see sections 5j and 6h, respectively). Low winter/spring polar ozone is a consequence of stable and cold stratospheric winter vortices with very low temperatures that permit wide-spread formation of polar stratospheric clouds (PSC), chlorine activation, and large polar ozone depletion (Solomon et al. 1999, 2015).

Figure 2.57 shows time series of Arctic and Antarctic daily minimum total column ozone. Generally, Arctic minimum total ozone increases from early winter (November) to spring (April). However, in cold Arctic winters, with stratospheric temperatures sufficiently low for persistent PSC formation (~195 K), minimum total ozone decreases over the winter, due to both chemical loss and reduced poleward ozone transport related to a weak Brewer-Dobson circulation (BDC; Lawrence et al. 2020). In March 2020 record low column values slightly below 220 Dobson unit (DU) were reached (Inness et al. 2020, Dameris et al. 2021), less than in previous cold winters (e.g., 2010/11). Even these record minimum values are, however, higher than values observed in the Southern Hemisphere (SH) ozone hole. Chemical ozone losses of up to 2.8 ppm near 18 km altitude and 88 DU (vortex average) by the end of March 2020 were similar to losses observed in March 2011, but due to the larger polar vortex area, the ozone mass loss was higher in 2020 and reached a new record after the previous record in 2011 (Manney et al. 2020; Weber et al. 2021). Without the Montreal Protocol phaseout of ODS, this chemical ozone loss would have been even higher (Feng et al. 2021). Above Antarctica, minimum total column ozone remained extremely low in 2020 and only rose rapidly at the end of November about 2 months later than in 2016, which had a winter with an average size ozone hole.

The low total ozone levels during winter/spring in both hemispheres contributed significantly to the annual mean low ozone anomaly (Plate 2.1aa). Zonally averaged annual mean total column ozone was as much as 20 and 60 DU below the long-term mean of 1998–2008 at northern middle and Arctic latitudes, respectively. The band of positive anomalies in the outer tropics along with

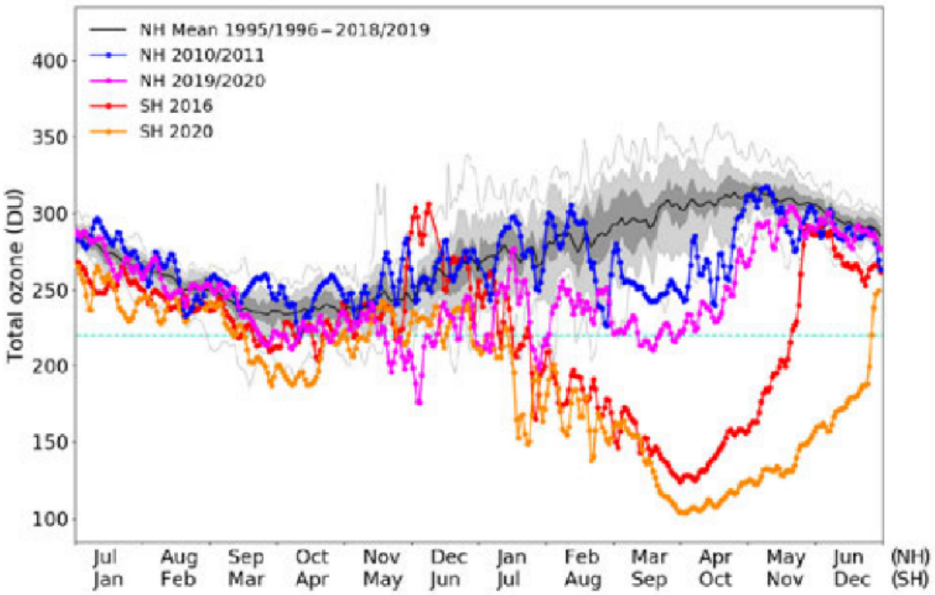

Fig. 2.57. Annual cycle of daily minimum total column ozone values (Dobson Units [DU]) in the polar regions between 50° and 90° in both hemispheres derived from the European GOME-type Total Ozone Essential Climate Variable (GTO) satellite record from Jul 1995 to Jun 2019 and TROPOMI data thereafter. The black line shows the GTO mean annual cycle in the north polar region. The thin gray lines indicate the maximum and minimum values of the observed daily minima from Jul 1995 to Jun 2019. The light gray shading denotes the 10th percentile and 90th percentile, the dark gray shading the 30th percentile and 70th percentile, respectively. The cyan dashed line shows the upper limit of 220 DU that defines the edge of the Antarctic ozone hole. Total ozone minimum time series are shown for winter/spring 2010/11 (blue) and 2019/20 (magenta) in the Northern Hemisphere (Jul–Jun) and in Antarctic winter/spring 2016 (red) and 2020 (orange) in the Southern Hemisphere (Jan–Dec). Updated from Dameris et al. (2021).

the negative anomalies at high latitudes are a typical pattern during quasi-biennial oscillation (QBO) westerly phases, as explained in previous reports. The Arctic Oscillation (AO) index was at a record high during Northern Hemisphere (NH) winter/spring and contributed to the very low ozone observed in the NH extratropics resulting from a very weak meridional circulation (Lawrence et al. 2020).

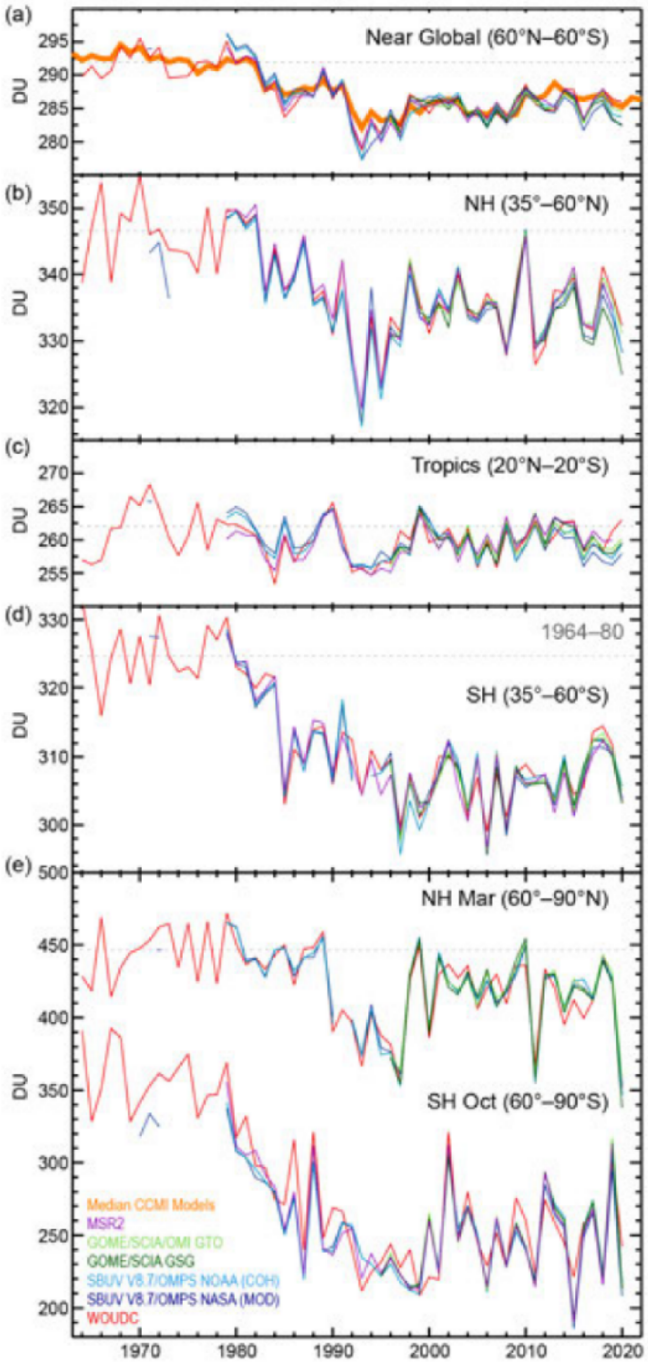

Figure 2.58 shows the long-term evolution of total column ozone for different zonal bands. Except for the polar region (NH: March mean; SH: October mean) annual mean total column ozone is shown. Following the decline until the middle 1990s due to ODS increases, total column ozone has remained at a steady level with substantial year-to-year variability during the last 2 decades, but still well below the 1964–80 mean (indicated by the dashed line). Near-global mean total column ozone (Fig. 2.58a) is on average still about 2% below the 1964–80 mean. The median ozone from the Chemistry Climate Model Initiative (CCMI) model simulations (SPARC/IO3C/GAW 2019), accounting for ODS and greenhouse gas changes, is in good agreement with observations. This shows that ozone observations are consistent with the expected slow ozone recovery due to the phasing out of certain ODSs (section 2g2). In 2020, the annual means in all latitude bands, as well as the Arctic March and Antarctic October mean (Fig. 2.58), were all below the decadal average of 1998–2008, but were within the variability observed in recent years (except March 2020).

Figure 2.59 shows the ozone evolution at different altitudes in the stratosphere. Ozone in the upper stratosphere showed a large decline in the 1980s caused by ODS increases, which was stopped in the late 1990s, thanks to the ODS phase-out mandated by the Montreal Protocol. Since about 2000, upper stratospheric ozone has been in a phase of slow recovery. In

Fig. 2.58. Time series of annual mean total column ozone (Dobson Units [DU]) in (a)–(d) four zonal bands, and (e) polar (60°–90°) total column ozone in Mar (Northern Hemisphere) and Oct (Southern Hemisphere), the months when polar ozone losses usually are largest. Red: WOUDC ground-based measurements combining Brewer, Dobson, SAOZ, and filter spectrometer data (Fioletov et al. 2002, 2008). Dark blue and light blue: BUV/SBUV/SBUV2 V8.6/OMPS merged products from NASA (MOD V8.6, Frith et al. 2014, 2017) and NOAA (Wild and Long, personal communication, 2019), respectively. Dark green and light green: GOME/SCIAMACHY/GOME-2 products GSG from University of Bremen (Weber et al. 2018) and GTO (additionally includes OMI and TROPOMI) from ESA/DLR (Coldewey-Egbers et al. 2015; Garane et al. 2018). Purple: MSR-2, which assimilates nearly all available ozone datasets after corrections based on the ground-based data (van der A et al. 2015). All datasets have been bias-corrected by subtracting averages for the reference period 1998–2008 and adding back the mean of these averages. The dashed gray lines in each panel show the average ozone level for 1964–1980 calculated from the WOUDC data. The thick orange line shows the median from CCMI model runs (SPARC/IO3C/GAW, 2019). Most of the observational data for 2020 are preliminary.

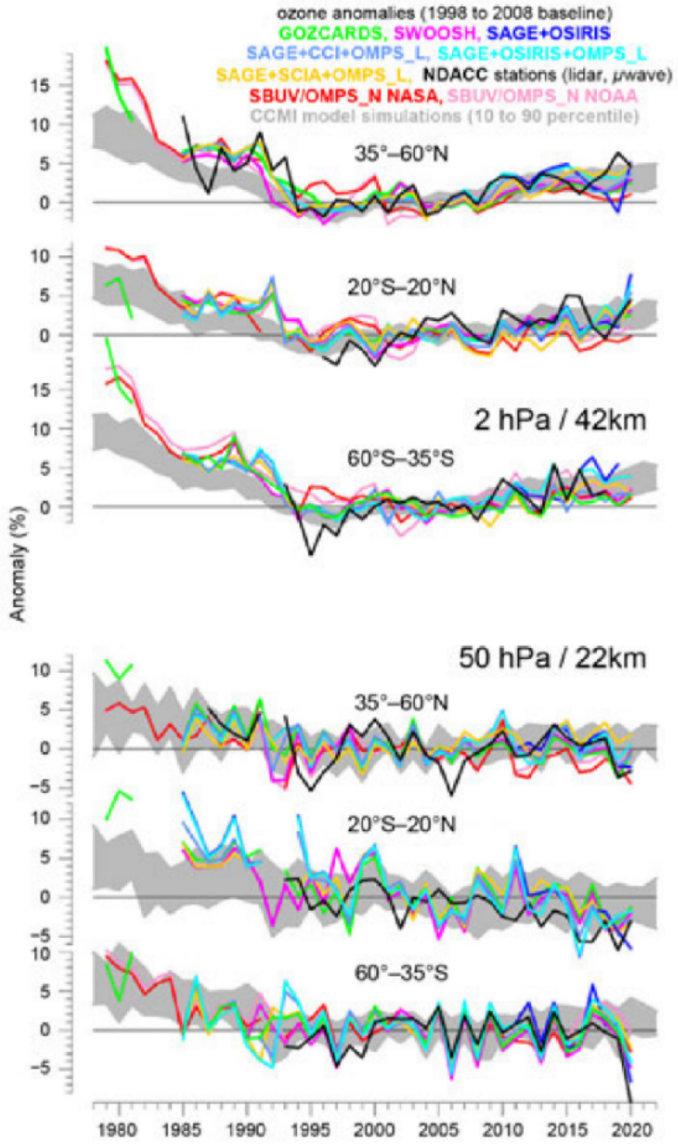

Fig. 2.59. Annual mean anomalies of ozone in the upper stratosphere (top three panels) near 42-km altitude or 2-hPa pressure, and in the lower stratosphere (bottom three panels, near 22 km or 50 hPa for three zonal bands: 35°–60°N, 20°S–20°N (tropics), 35°–60°S respectively. Anomalies are referenced to the 1998–2008 baseline. Colored lines are long-term records obtained by merging different limb (GOZCARDS, SWOOSH, SAGE+OSIRIS, SAGE+CCI+OMPS-L, SAGE+SCIAMACHY+OMPS-L, SAGE+OSIRIS+OMPS-L) or nadir-viewing (SBUV, OMPS-N) satellite instruments. The nadir-viewing instruments have much coarser altitude resolution than the limb-instruments. This can cause differences in some years, especially at 50 hPa. The black line is from merging ground-based ozone records at seven NDACC stations employing differential absorption lidars and microwave radiometers. See Steinbrecht et al. (2017), WMO (2018), and Arosio et al. (2018) for details on the various datasets. Gray-shaded area shows the range of simulations from CCMI (SPARC/IO3C/GAW 2019). At the time of publication, ozone data for 2020 were not yet complete for all instruments and were still preliminary.

all recent years, including 2020, ozone values in the upper stratosphere from most datasets were above the 1998–2008 average, consistent with expectations from the CCMI simulations (gray shaded range in Fig. 2.59; SPARC/IO3C/GAW 2019). In the lower stratosphere, however, long-term ozone variations are dominated by meteorological and transport variations (e.g., Chipperfield et al. 2018), and Fig. 2.59 shows no clear sign of ozone increases in this region over the last 20 or so years. This is consistent with total column ozone in Fig. 2.58. In 2020, lower stratospheric values were at the low end of recent years, and also at the low end of the model predictions. The tropical (20°S–20°N) long-term ozone decline is linked to the acceleration of the meridional Brewer-Dobson circulation (Ball et al. 2018; Chipperfield et al. 2018; WMO 2018). The low annual mean 2020 values of lower stratospheric ozone in the northern and southern extratropical 35°–60° latitude bands, however, similar to the generally low total column ozone (Plate 2.1aa; Fig. 2.58), are the result of the weak meridional Brewer-Dobson circulation in winter in both hemispheres.

5) Stratospheric water vapor—S. M. Davis, K. H. Rosenlof, D. F. Hurst, and H. Vömel

Variations in stratospheric water vapor (WV) occur over a wide range of timescales and can impact stratospheric ozone (Dvortsov and Solomon 2001) and surface climate (Solomon et al. 2010). Such variations are forced by prominent modes of seasonal and interannual dynamical variability that influence temperatures in the tropical tropopause layer (TTL; ~14–19 km). In general, the amount of WV entering the stratosphere is controlled by the lowest temperature encountered by an ascending air mass (i.e., through the Clausius-Clapeyron relationship), with more WV entering the stratosphere when TTL temperatures are warmer. As a result, processes that cause temporal variability in TTL temperatures also lead to global-scale variability in stratospheric WV.